

Spin-Orbit Effects on Structures of Closed-Shell Polyatomic Molecules Containing Heavy Atoms Calculated by Two-Component Hartree–Fock Method

YOUNG-KYU HAN,¹ CHEOLBEOM BAE,¹ YOON SUP LEE,¹
SANG YEON LEE²

¹Department of Chemistry, Korea Advanced Institute of Science and Technology, Taejeon 305-701, Korea

²Department of Industrial Chemistry, Kyungpook National University, Taegu, Korea

Received 3 March 1998; accepted 11 May 1998

ABSTRACT: We have implemented geometry optimization using an analytic gradient to a two-component Kramers' restricted Hartree–Fock (KRHF) method for polyatomic molecules with closed-shell configurations. The KRHF method is a Hartree–Fock method based on relativistic effective core potentials with effective spin-orbit operators. The derivatives of spin-orbit integrals are obtained by numerical differentiation. Geometries for the various forms of polyatomic hydrides containing row 6 p-block elements are optimized with and without spin-orbit interactions. The structural changes due to spin-orbit interactions are small, but show definite trends, which correlate well with the $p_{1/2}$ spinor population. Atomization energies are reduced significantly by incorporating spin-orbit interactions for all molecules considered. The KRHF calculations of several methylhalides demonstrate that the spinor energies from the KRHF method can be useful for the interpretation of experimental photoelectron spectra of molecules exhibiting spin-orbit splittings. © 1998 John Wiley & Sons, Inc. *J Comput Chem* 19: 1526–1533, 1998

Keywords: geometry optimization; spin-orbit effect; two-component calculation; effective core potential with one-electron spin-orbit operator; photoelectron spectra

Correspondence to: Y. S. Lee; e-mail: yslee@xe1.kaist.ac.kr

Contract/grant sponsors: Korea Research Foundation;
STEPI-MOST

Introduction

Relativistic effective core potential (RECP) methods are probably the most successful approximation methods for the various properties of molecules containing heavy atoms because RECP calculations can economically yield results very close to all-electron results without introducing any empirical parameters.^{1–4} Because spin-orbit interactions are included in the relativistic representation of electrons, many variants of RECP contain spin-orbit interactions. Even with these spin-orbit RECP's, the popular approaches start with spin-averaged relativistic effective core potential (AREP) at the HF level, which is identical to the conventional nonrelativistic method in the formalism. Spin-orbit terms can be introduced, if desired, at post-HF steps.^{5–8} Another approach for the use of two-component spinors, in which RECPs including spin-orbit interactions are treated from the HF step, is not as widely used, partly due to the additional complexity in computation, but may have advantages in some cases.^{9–13} First, it is simple to obtain spin-orbit effects in geometries, energies, and properties at the HF level. Second, two-component RECP results are directly comparable with those of corresponding Dirac–Hartree–Fock (DHF) calculations. This direct comparison can be used to assess the validity of the various approximations inherent in RECP calculations. In addition, when the spin-orbit effects are substantial, it may be possible to recover larger portions of the electron correlation energies from the post-HF calculations based on the reference state generated in the presence of spin-orbit interactions versus those neglecting spin-orbit interactions. To investigate these characteristics using calculations for molecules containing heavy atoms, we have developed various electronic structure codes starting from the two-component HF method using RECP methods such as Möller–Plesset second-order perturbation (MP2), configuration interaction (CI), and coupled cluster (CC) methods. We refer to our restricted HF method as KRHF and the corresponding MP2, CI, and CC as KRMP2, KRCI, and KRCC, respectively,^{9–13} because one-electron wave functions are described by two-component spinors, confirming Kramer degeneracy.

In the present work, we have implemented geometry optimization in the KRHF program using first derivative integrals. We calculate all deriva-

tive integrals analytically, but the derivatives of spin-orbit integrals are obtained by numerical differentiation. To the best of our knowledge, there have been no attempts to optimize molecular structures using analytic gradient in calculations with spin-orbit interactions. Reported relativistic studies on polyatomic molecules have been mainly restricted to dimers, symmetric trimers, or larger polyatomic molecules with high symmetries such as T_d or O_h symmetry. The present work will open an avenue to study spin-orbit effects on the structures of polyatomic molecules with low symmetries.

Spin-orbit effects on geometries and atomization energies have been calculated at the HF level of theory using RECPs for thallium hydrides, lead hydrides, and M_2H_2 ($M = \text{Pb, Bi, and Po}$) molecules and the results are given in the following sections. In addition, RECP calculations of CH_3X and CX_4 ($\text{X} = \text{Br, I, and At}$) molecules demonstrate that orbital energies can be valuable in the interpretation of photoelectron spectra for polyatomic molecules containing heavy atoms.

Method

For a polyatomic molecule with n_v valence electrons, the two-component molecular electronic Hamiltonian¹⁴ can be expressed (in atomic units) as

$$H = \sum_{i=1}^{n_v} h(i) + \sum_{i>j}^{n_v} \frac{1}{r_{ij}} \quad (1)$$

$$h(i) = -\frac{1}{2}\nabla_i^2 + \sum_{a=1}^N \left(-\frac{Z_a^{\text{eff}}}{r_{ai}} + U_a^{\text{REP}} \right) \quad (2)$$

where i and j denote valence electrons, a is a core index, Z_a^{eff} is the charge of core a , and U_a^{REP} is the RECP of atom a . There can be many variations in the form of RECPs and the present RECP (REP) is expressed in the form¹⁵

$$\begin{aligned} U^{\text{REP}} = & U_L^{\text{REP}}(r) \\ & + \sum_{l=0}^{L-1} \sum_{j=|l-\frac{1}{2}|}^{l+\frac{1}{2}} \sum_{m=-j}^j \left[U_{lj}^{\text{REP}}(r) - U_L^{\text{REP}}(r) \right] \\ & \times |ljm\rangle\langle ljm| \end{aligned} \quad (3)$$

where $|ljm\rangle\langle ljm|$ represents a two-component projection operator. Molecular spinors that are one-electron eigenfunctions of the REP of eq. (2) have two components. The U^{REP} of eq. (2), which is

referred to as REP here for distinction from other types of RECPs in the literature, can be expressed as the sum of the weighted average of AREP (AREP), U^{AREP} , and the effective one-electron spin-orbit (ESO) operator,¹⁵ U^{SO} , as

$$U^{REP} = U^{AREP} + U^{SO} \quad (4)$$

In eq. (4), the AREP has the form

$$U^{AREP} = U_L^{AREP}(r) + \sum_{l=0}^{L-1} \sum_{m=-l}^l [U_l^{AREP}(r) - U_L^{AREP}(r)] \times |lm\rangle\langle lm| \quad (5)$$

where

$$U_l^{AREP}(r) = \frac{1}{2l+1} \times [l \cdot U_{l,l-\frac{1}{2}}^{REP}(r) + (l+1)U_{l,l+\frac{1}{2}}^{REP}(r)] \quad (6)$$

and the ESO can be written

$$U^{SO} = \mathbf{s} \cdot \sum_{l=1}^L \frac{2}{2l+1} \Delta U_l^{REP}(r) \times \sum_{m=-l}^l \sum_{m'=-l}^l |lm\rangle\langle lm||lm'\rangle\langle lm'| \quad (7)$$

where

$$\Delta U_l^{REP}(r) = U_{l,l+\frac{1}{2}}^{REP}(r) - U_{l,l-\frac{1}{2}}^{REP}(r) \quad (8)$$

When ESO is omitted in eq. (3), REP is reduced to AREP that is equivalent in form to many effective core potentials in the conventional relativistic method. The use of AREP in the conventional molecular orbital calculation is known to produce most relativistic effects except for the spin-orbit effects. Spin-orbit effects can be investigated by performing additional calculations with and without ESO at various levels.

The two-component Hamiltonian of eq. (1) is invariant under the time reversal operation. In the one-electron case, and for a special choice of phases, time reversal operator, T , is given by

$$T = -i\sigma_y T_0 \quad (9)$$

where σ_y is the Pauli matrix acting on the spin part of the spinor and T_0 is the complex conjugation operator for the orbital part. Kramers' symmetry leaves the spinor pair $(\psi, T\psi)$ degenerate. The

total wave function can then be written in terms of Kramers' restricted spinor pairs as

$$\Psi = \hat{A} |\phi_1(T\phi_1)\phi_2(T\phi_2) \cdots \phi_{n_v/2}(T\phi_{n_v/2})| \quad (10)$$

and the total electronic energy is

$$E_e = 2 \sum_i^{n_v/2} h_i + \sum_{i,j}^{n_v/2} (2J_{ij} - K_{ij} - L_{ij}) \quad (11)$$

where

$$J_{ij} = \langle \phi_i | J_j | \phi_i \rangle = \langle \phi_i \phi_j | \frac{1}{r_{12}} | \phi_i \phi_j \rangle \quad (12)$$

$$K_{ij} = \langle \phi_i | K_j | \phi_i \rangle = \langle \phi_i \phi_j | \frac{1}{r_{12}} | \phi_j \phi_i \rangle \quad (13)$$

$$L_{ij} = \langle \phi_i | L_j | \phi_i \rangle = \langle \phi_i T\phi_j | \frac{1}{r_{12}} | T\phi_j \phi_i \rangle \quad (14)$$

As in the nonrelativistic case, all one-electron molecular spinors are expressed in terms of orbital basis and spin functions

$$\psi_i = \sum_p c_{ip\alpha} \chi_p \alpha + \sum_p c_{ip\beta} \chi_p \beta \quad (15)$$

where α and β refer to spin functions and χ_p is a basis function. The energy gradient with respect to energy expression of eq. (11) is

$$E'_e = 2 \sum_i^{n_v/2} h'_i + \sum_{i,j}^{n_v/2} (2J'_{ij} - K'_{ij} - L'_{ij}) - 2 \sum_i^{n_v/2} \varepsilon_i S'_i \quad (16)$$

where ε_i is i th spinor energy. Eq. (16) is formally equivalent to the nonrelativistic case except for the L' term. Because no new features due to the two-component nature are necessary to calculate gradients, detailed expressions of the energy derivative are omitted. All derivative integrals except spin-orbit terms are obtained from a modified version of the GAMESS suite of program.¹⁶ Because the code to calculate analytical derivatives of spin-orbit integrals is not available, we obtain the required integrals by numerically differentiating spin-orbit integrals from the ARGOS code^{17,18} of the COLUMBUS package.¹⁹ The routine to optimize structures using gradients is also taken from the COLUMBUS package.^{20,21}

Computational Details

The Gaussian-94 package²² and the KRHF code are used for HF calculations using AREPs and HF calculations using REPs, respectively, on the Cray C90 at SERI. The RECPs used here are the spin-averaged AREPs and the REPs including spin-orbit terms provided by Christiansen, Emler, and their coworkers (CE).^{23–28} The RECPs of CE are convenient to study the relativistic effects and have been utilized in many studies of spin-orbit effects.²⁹ The notation n_v -e is used to denote RECP of an atom in which n_v valence electrons are explicitly retained in the generation of RECP. The semicore RECPs (d electrons in valence) 13-e Tl, 14-e Pb, 15-e Bi, and 16-e Po, are used for thallium hydrides, lead hydrides, and M_2H_2 ($M = \text{Tl, Pb, Bi, and Po}$) molecules with the basis sets recommended by CE in uncontracted forms. The full-core RECPs (d electrons in core) are used for CH_3X and CX_4 ($\text{X} = \text{Br and I}$) with uncontracted CE basis sets and the 17-e At RECP is used for the molecules containing the At atom with the $[5s5p5d/4s4p2d]$ basis set. All-electron 6-311G** basis sets are used for carbon and hydrogen atoms. Calculated molecular properties are equilibrium bond lengths and atomization energies using AREPs and REPs. REP results of Mulliken population analysis are also calculated by the KRHF code. The ground state energies of atoms with REP, which are required to evaluate atomization energies, have been calculated using the JJAHF program.³⁰

Results and Discussion

Spinor Mulliken populations and Tl–H bond lengths for some thallium hydrides are summarized in Table I. Tl_2H_2 has the D_{2h} di-H-bridged structure as previously reported (Fig. 1).^{31,32} We did not find any additional minimum structure for Tl_2H_2 at the HF level. Spin-orbit interactions contract the Tl–H bonds slightly in all cases by 0.01–0.05 bohr. The all-electron density functional theory (DFT) calculation for TIH using zero-order regular approximation (ZORA) predicted the contraction by 0.059 bohr.³³ Schwerdtfeger et al.³⁴ obtained ΔR_{SO} of -0.008 bohr in the ARPP/QRPP^{35,36} calculations, which is much smaller in magnitude than the -0.051 bohr predicted by the present calculation or the DFT value. The $|\Delta R_{SO}|$ values decrease as the number of hydrogen atoms increases, which is in line with the trend that the population ratio, $p_{3/2}/p_{1/2}$, becomes close to the AREP limit value of 2.0 for a large number of hydrogen atoms. For Tl_2H_2 , the Tl–Tl bonding does not exist at the HF level of theory as was pointed out by Schwerdtfeger³¹ and four Tl–H bonds contract due to spin-orbit effects by 0.034 bohr. The $|\Delta R_{SO}|$ and $p_{3/2}/p_{1/2}$ values in Tl_2H_2 are intermediate between those in TIH and in TIH_2^+ , as one might expect.

The results of lead hydrides are listed in Table II. The changes of ΔR_{SO} and population ratios from PbH^+ to PbH_4 are similar to thallium hy-

TABLE I. Spinor Populations and Tl—H Bond Lengths of Thallium Hydrides Calculated by HF and KRHF Methods.^a

| | Sym. | s | $p_{1/2}$ | $p_{3/2}$ | $p_{3/2}/p_{1/2}$ | R_e | ΔR_{SO} |
|---------------------------|----------------|-------|-----------|-----------|-------------------|-------|-----------------|
| TIH | $C_{\infty v}$ | 1.895 | 0.260 | 0.519 | 2.00 | 3.578 | |
| | | 1.884 | 0.454 | 0.364 | 0.80 | 3.527 | -0.051 |
| TIH_2^+ | $D_{\infty h}$ | 1.417 | 0.237 | 0.474 | 2.00 | 3.118 | |
| | | 1.416 | 0.344 | 0.379 | 1.10 | 3.108 | -0.010 |
| TIH_3 | D_{3h} | 1.186 | 0.430 | 0.861 | 2.00 | 3.272 | |
| | | 1.184 | 0.560 | 0.751 | 1.34 | 3.262 | -0.010 |
| TIH_4^+ | D_{4h} | 1.273 | 0.485 | 0.970 | 2.00 | 3.108 | |
| | | 1.272 | 0.608 | 0.861 | 1.42 | 3.101 | -0.007 |
| Tl_2H_2^b | D_{2h} | 1.923 | 0.216 | 0.432 | 2.00 | 4.083 | |
| | | 1.919 | 0.326 | 0.346 | 1.06 | 4.049 | -0.034 |

^a For each molecule, the first (second) row refers to AREP (REP) results. Units are in bohr.

^b Molecular geometries are shown in Figure 1.

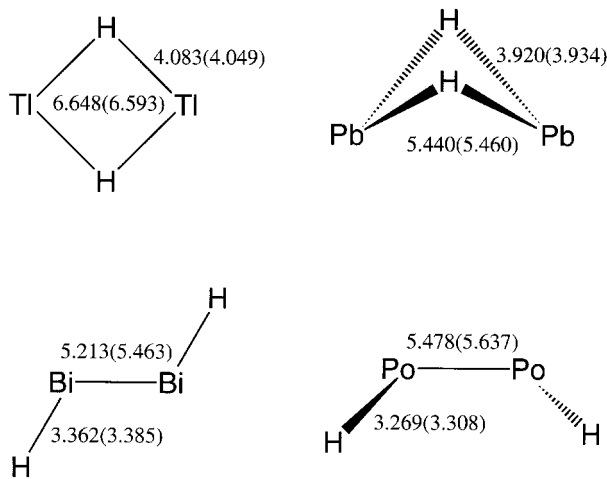


FIGURE 1. AREP (REP)-optimized geometries of M_2H_2 ($M = \text{Ti, Pb, Bi, and Po}$) molecules. AREP (REP) angles are as follows: $\angle(\text{HTlTi}) = 35.5$ (35.5); $\angle(\text{HPbPb}) = 46.1$ (46.1); $\tau(\text{HPbPbH}) = 107.6$ (105.1); $\angle(\text{HBiBi}) = 91.7$ (91.4); $\angle(\text{HPoPo}) = 95.0$ (94.9); $\tau(\text{HPoPoH}) = 89.7$ (89.9).

dride cases. According to Dyall,³⁷ the spin-orbit effect on the angle of PbH_2 estimated as the deviation of the perturbation theory (PT) value from the DHF one is $+0.8^\circ$, which is in good agreement with our value of $+0.8^\circ$. Schwerdtfeger et al.³⁸ obtained a spin-orbit effect of -1.3° for the PbH_2 bond angle. Dyall³⁷ pointed out that the large-core pseudopotentials used by Schwerdtfeger et al. may have described the spin-orbit effects incorrectly. The ARPP/QRPP calculations by Steinbrenner et al.³⁹ showed that ΔR_{SO} is -0.04 bohr for PbH_4 ,

which is similar to our result of -0.006 bohr. The REP bond lengths for PbH_2 and PbH_4 are 3.464 and 3.284 bohr, respectively, in good agreement with the DHF bond lengths of 3.434 and 3.292 bohr.^{37, 40}

Unlike the case of Ti_2H_2 , direct Pb—Pb bonding exists for Pb_2H_2 . The occupancy of the bond from the natural bond orbital analysis is 1.99 in the AREP calculation. The ΔR_{SO} of the Pb—H bond ($+0.014$ bohr) for Pb_2H_2 , which deviates from the trend of other lead hydrides, may be due to the directly bonding Pb atoms. We confirmed that ΔR_{SO} is negative, which is in line with other lead hydrides, when the $\angle(\text{PbPbH})$ angle becomes obtuse. In fact, all M—H and M—M bond lengths are elongated by spin-orbit effects for M_2H_2 ($M = \text{Pb, Bi, and Po}$), as shown in Figure 1. The M—H bond lengths increase by 0.01–0.04 bohr and M—M bond lengths are elongated by 0.020, 0.250, and 0.159 bohr for $M = \text{Pb, Bi, and Po}$, respectively. The changes of angles due to spin-orbits effects are found to be very small, and the values are listed in the caption to Figure 1.

Atomization energies of thallium and lead hydrides are shown in Table III. Spin-orbit effects on the total energies of molecules are generally small, but the energies of atoms composing molecules are significantly lowered for the atoms with open shells of p or higher angular momentum valence electrons. As a result, atomization energies are reduced significantly by the lowered atomic limit, as shown in Table III. The small increase of ΔA_e (SO) in TiH_2^+ and TiH_4^+ is due to the fact that the

TABLE II. Spinor Populations and Pb — H Bond Lengths of Lead Hydrides Calculated by HF and KRHF Methods.^a

| | Sym. | s | p _{1/2} | p _{3/2} | p _{3/2} p _{1/2} | R _e | ΔR_{SO} |
|---|-----------------|-------|------------------|------------------|-----------------------------------|----------------|------------------------|
| PbH ⁺ | C _{∞v} | 1.926 | 0.316 | 0.632 | 2.00 | 3.427 | |
| | | 1.914 | 0.647 | 0.361 | 0.56 | 3.389 | −0.038 |
| PbH ₂ ^b | C _{2v} | 1.828 | 0.563 | 1.126 | 2.00 | 3.464 | |
| | | 1.815 | 0.833 | 0.904 | 1.09 | 3.440 | −0.024 |
| PbH ₃ ⁺ | D _{3h} | 1.415 | 0.549 | 1.097 | 2.00 | 3.239 | |
| | | 1.411 | 0.729 | 0.941 | 1.29 | 3.229 | −0.010 |
| PbH ₄ | T _d | 1.281 | 0.700 | 1.401 | 2.00 | 3.288 | |
| | | 1.278 | 0.813 | 1.305 | 1.61 | 3.282 | −0.006 |
| Pb ₂ H ₂ ^c | C _{2v} | 1.943 | 0.574 | 1.148 | 2.00 | 3.920 | |
| | | 1.943 | 1.036 | 0.717 | 0.69 | 3.934 | +0.014 |

^a For each molecule, the first (second) row refers to AREP (REP) results. Units are in bohr.
^b The AREP (REP) angle for PbH_2 is 91.6 (92.4) deg.
^c Molecule shown in Figure 1.

TABLE III.
Atomization Energies (A_e) of Thallium Hydrides and Lead Hydrides Calculated by HF and KRHF Methods (Units in eV).

| | Sym. | AREP | REP | ΔA_{SO}^a |
|-----------|----------------|------|------|-------------------|
| TlH^b | $C_{\infty v}$ | 1.67 | 1.14 | -0.53 |
| TlH_2^+ | $D_{\infty h}$ | 1.52 | 1.66 | +0.14 |
| TlH_3 | D_{3h} | 4.53 | 4.03 | -0.50 |
| TlH_4^+ | D_{4h} | 1.10 | 1.32 | +0.22 |
| Tl_2H_2 | D_{2h} | 3.98 | 2.81 | -1.17 |
| PbH^+ | $C_{\infty v}$ | 1.62 | 0.74 | -0.88 |
| PbH_2 | C_{2v} | 3.19 | 2.35 | -0.84 |
| PbH_3^+ | D_{3h} | 4.01 | 3.08 | -0.93 |
| PbH_4 | T_d | 6.57 | 5.67 | -0.90 |
| Pb_2H_2 | C_{2v} | 3.80 | 2.36 | -1.44 |

^a $\Delta A_{SO} = A_e(\text{REP}) - A_e(\text{AREP})$.^b Experimental value 2.06 eV.⁴²

asymptote is the Tl^+ ion with closed-shell electronic structure. Spin-orbit-induced stabilization will be more evident for molecules composed of atoms not having open p shells such as Au, Hg, and Rn.⁴¹ The dissociation energy of the TlH molecule is known to be 2.06 eV,⁴² indicating the importance of electron correlations for a reasonable description of dissociation energy. Although the present atomization energy is not accurate, the present scheme offers a good estimate of spin-orbit effects on atomization energies. The spin-orbit effects on the bond stability for some thallium hydrides were studied by Schwerdtfeger et al.⁴³ and their results are in general agreement with the present results.

The valence orbital energies from HF and KRHF calculations for CH_3X and CX_4 ($X = Br, I$, and At) are presented in Tables IV and V, respectively, with available experimental photoelectron spectroscopy (PES) data. The orbital energies are obtained at fully optimized equilibrium geometries. Spin-orbit interactions elongate the $C-X$ bond lengths of the CH_3X molecules by 0.001, 0.005, and 0.057 bohr for CH_3Br , CH_3I , and CH_3At , respectively. The changes of $C-H$ bond lengths and $H-C-X$ angles due to spin-orbit effects are negligible. Calculated spin-orbit splittings for the outermost valence e orbitals of CH_3Br and CH_3I are 0.35 and 0.69 eV, respectively, which are in good agreement with experimental values of 0.28 and 0.62 eV, respectively.⁴⁴ The spin-orbit splitting for the outermost e orbital of CH_3At can be estimated to be about 1.53 eV from the REP calculation. Spin-orbit interactions also elongate the $C-X$

TABLE IV.
Orbital Energies from HF and KRHF Calculations at Optimized Geometries^a and Ionization Potentials from PES for Methylhalides (Units in eV).

| | AREP | REP | Exp ^b |
|----------|--------|----------------|------------------|
| CH_3Br | | | |
| e | -10.81 | -10.63, -10.98 | -10.53, -10.85 |
| a | -13.70 | -13.71 | -13.52 |
| e | -16.71 | -16.70, -16.72 | -15.14 |
| CH_3I | | | |
| e | -9.72 | -9.36, -10.05 | -9.54, -10.16 |
| a | -12.52 | -12.60 | -12.50 |
| e | -16.54 | -16.51, -16.53 | -14.80 |
| CH_3At | | | |
| e | -9.31 | -8.34, -9.87 | |
| a | -11.93 | -12.80 | |
| e | -16.52 | -16.31, -16.36 | |

^a The optimized AREP (REP) geometries of methylhalides are as follows (r in bohr and angles in degrees): $r(C-Br) = 3.668$ (3.669), $r(C-H) = 2.036$ (2.036), and $\angle(Br-C-H) = 107.7$ (107.7) for CH_3Br ; $r(C-I) = 4.058$ (4.063), $r(C-H) = 2.035$ (2.036), and $\angle(I-C-H) = 107.5$ (107.5) for CH_3I ; and $r(C-At) = 4.273$ (4.330), $r(C-H) = 2.034$ (2.035), and $\angle(At-C-H) = 106.8$ (106.7) for CH_3At .

^b Ref. 44.**TABLE V.**
Orbital Energies from HF and KRHF Calculations and Ionization Potentials from PES for Carbon Tetrahalides (Units in eV).^a

| | AREP | REP | Exp ^a |
|---------|--------|-------------------|------------------|
| CBr_4 | | | |
| t_1 | -11.16 | -11.04(2), -11.39 | -10.60 |
| t_2 | -11.89 | -11.67(2), -12.33 | -11.30 |
| e | -12.95 | -12.94(2) | -12.10 |
| t_2 | -16.33 | -16.18, -16.41(2) | -15.00 |
| Cl_4 | | | |
| t_1 | -9.72 | -9.46(2), -10.24 | -9.15, -9.84 |
| t_2 | -10.38 | -9.94(2), -11.25 | -9.58, -10.76 |
| e | -11.34 | -11.31(2) | -10.75 |
| t_2 | -14.37 | -13.98, -14.54(2) | -13.09, -13.45 |
| CAt_4 | | | |
| t_1 | -9.21 | -8.36(2), -11.26 | |
| t_2 | -9.75 | -8.47(2), -12.04 | |
| e | -10.65 | -10.38(2) | |
| t_2 | -13.49 | -12.43, -14.28(2) | |

^a Degeneracy numbers in parentheses.

^b Ref. 48 for CBr_4 and ref. 45 for Cl_4 . The optimized AREP (REP) bond lengths of carbon tetrahalides are 3.650 (3.652), 4.092 (4.103), and 4.314 (4.399) bohr for CBr_4 , Cl_4 , and CAt_4 , respectively.

bond lengths in the CX_4 molecules by 0.002, 0.011, and 0.085 bohr for CBr_4 , CI_4 , and CAt_4 , respectively. Experimental PES data with spin-orbit splittings for CI_4 have been reported.⁴⁵ Calculated spin-orbit splittings for the outermost t1 and t2 orbitals for CI_4 were found to be 0.78 and 1.31 eV, respectively, which are also in good agreement with experimental values of 0.69 and 1.18 eV. Roszak et al.⁴⁶ assigned first (I), third (II), and fourth (III) experimental peaks with their theoretical values taken from the MRD-RCI calculations of CI_4^+ . Their $\Delta E(E(II) - E(I))$ and $\Delta E(E(III) - E(I))$ values of 0.52 and 1.56 eV, respectively, are in good agreement with our results (0.48 and 1.79 eV) as well as experimental values (0.43 and 1.61 eV). It should be noted that our REP results describe qualitatively the PES peaks of CI_4 at the HF level of theory. The orbital energies of CAt_4 are also listed in Table V. The spin-orbit splittings of the CAt_4 molecule are two to three times larger than those of the CI_4 case. The outermost two peaks originating from t1 and t2 orbitals are almost degenerate near 8.41 eV due to spin-orbit splittings. These peaks are difficult to assign without the aid of theoretical calculations, and the present KRHF is probably the simplest *ab initio* approach that allows vertical ionization potentials for molecules exhibiting spin-orbit splittings.

Conclusions

We have implemented geometry optimization using an analytic gradient to the KRHF method, which treats spin-orbit interactions at the HF level of theory. This allows us to optimize molecular structures of low symmetries with and without spin-orbit interactions. The geometries for various forms of polyatomic molecules, thallium hydrides, lead hydrides, and M_2H_2 ($M = Tl, Pb, Bi, \text{ and } Po$) were optimized and the spin-orbit effects on the molecules have been discussed. Spin-orbit effects on the structures of the molecules containing row 6 elements were small but had definite trends that correlated well with the relative population in the $p_{1/2}$ atomic spinors. Previous work with row 6 metal hydrides has shown that bond lengths are generally contracted (elongated) when the bonding atomic spinors are $6p_{1/2}(6p_{3/2})$ spinors.⁴⁷ A similar trend was observed in the present work, except for Pb_2H_2 , for which bonding interactions between two Pb atoms competed with Pb—H bonds. The atomization energies were significantly reduced by

incorporating spin-orbit interactions when the asymptotic atoms involved p open shells. In other cases, atomization energies were increased slightly by the spin-orbit interactions.

From the calculations for CH_3X and CX_4 ($X = Br, I, \text{ and } At$) molecules, we demonstrated that the spinor energies from the KRHF method can be useful for the interpretation of photoelectron spectra of the molecules exhibiting spin-orbit splittings. We believe that the present work will lead to more systematic studies of spin-orbit effects on a variety of polyatomic molecules containing heavy and superheavy elements.

Acknowledgments

The authors are grateful to the authors of the COLUMBUS and GAMESS packages for making the source codes available.

References

1. M. Krauss and W. J. Stevens, *Ann. Rev. Phys. Chem.* **35**, 357 (1984).
2. P. A. Christiansen, W. C. Ermler, and K. S. Pitzer, *Ann. Rev. Phys. Chem.*, **36**, 407 (1985).
3. W. C. Ermler, R. B. Ross, and P. A. Christiansen, *Adv. Quant. Chem.*, **19**, 139 (1988).
4. K. Balasubramanian and K. S. Pitzer, *Adv. Phys. Chem.*, **87**, 287 (1987).
5. R. M. Pitzer and N. W. Winter, *J. Phys. Chem.*, **92**, 3061 (1988).
6. I. Boustani, S. N. Rai, H.-P. Liebermann, A. B. Alekseyev, G. Hirsch, and R. J. Buenker, *Chem. Phys.*, **177**, 45 (1993).
7. A. B. Alekseyev, H.-P. Liebermann, R. J. Buenker, G. Hirsch, and Y. Li, *J. Chem. Phys.*, **100**, 8956 (1994).
8. M. Vijayakumar, S. Roszak, and K. Balasubramanian, *Chem. Phys. Lett.*, **215**, 87 (1993).
9. S. Y. Lee and Y. S. Lee, *J. Comput. Chem.*, **13**, 595 (1992).
10. S. Y. Lee and Y. S. Lee, *Chem. Phys. Lett.*, **187**, 302 (1991).
11. M. C. Kim, S. Y. Lee, and Y. S. Lee, *Chem. Phys. Lett.*, **253**, 216 (1996).
12. H. S. Lee, Y. K. Han, M. C. Kim, C. Bae, and Y. S. Lee, *Chem. Phys. Lett.*, submitted.
13. Y. S. Kim, S. Y. Lee, W. S. Oh, B. H. Park, Y. K. Han, S. J. Park, and Y. S. Lee, *Int. J. Quant. Chem.*, **66**, 91 (1998).
14. Y. S. Lee, W. C. Ermler, and K. S. Pitzer, *J. Chem. Phys.*, **73**, 360 (1980).
15. W. C. Ermler, Y. S. Lee, P. A. Christiansen, and K. S. Pitzer, *Chem. Phys. Lett.*, **81**, 70 (1981).
16. M. W. Schmidt, K. K. Baldridge, J. A. Boatz, S. T. Elbert, M. S. Gordon, J. H. Jensen, S. Koseki, N. Matsunaga, K. A. Nguyen, S. J. Su, T. L. Windus, M. Dupuis, and J. A. Montgomery, GAMESS, Iowa State University, Ames, IA, 1995.

17. R. M. Pitzer is the principal author of this program that is part of the COLUMBUS suite of programs.
18. R. Shepard, I. Shavitt, R. M. Pitzer, D. C. Comeau, M. Pepper, H. Lischka, P. G. Szalay, R. Ahlrichs, F. B. Brown, and J. G. Zhao, *Int. J. Quant. Chem. Symp.*, **22**, 149 (1988).
19. H. Dachsel, H. Lischka, R. Shepard, J. Nieplocha, and R. J. Harrison, *J. Comput. Chem.*, **18**, 430 (1997).
20. P. G. Szalay is the author of this program that is part of the COLUMBUS suite of programs.
21. P. Csaszar and P. Pulay, *J. Mol. Struct.*, **114**, 31 (1984).
22. M. J. Frisch, G. W. Trucks, H. B. Schlegel, P. M. W. Gill, B. G. Johnson, M. A. Robb, J. R. Cheeseman, T. Keith, G. A. Petersson, J. A. Montgomery, K. Raghavachari, M. A. Al-Laham, V. G. Zakrzewski, J. V. Ortiz, J. B. Foresman, J. Cioslowski, B. B. Stefanov, A. Nanayakkara, M. Challacombe, C. Y. Peng, P. Y. Ayala, W. Chen, M. W. Wong, J. L. Andrews, E. S. Replogle, R. Gomperts, R. L. Martin, D. J. Fox, J. S. Binkley, D. J. Defrees, J. Baker, J. P. Stewart, M. Head-Gordon, C. Gonzalez, and J. A. Pople, *Gaussian-94, Revision B.2*, Gaussian, Inc., Pittsburgh, PA, 1995.
23. L. F. Pacios and P. A. Christiansen, *J. Chem. Phys.*, **82**, 2664 (1985).
24. M. M. Hurley, L. F. Pacios, and P. A. Christiansen, *J. Chem. Phys.*, **84**, 6840 (1986).
25. L. A. Lajohn, P. A. Christiansen, and R. B. Ross, *J. Chem. Phys.*, **87**, 2812 (1987).
26. R. B. Ross, J. M. Powers, T. Atashroo, W. C. Ermler, L. A. Lajohn, and P. A. Christiansen, *J. Chem. Phys.*, **93**, 6654 (1990).
27. W. C. Ermler, R. B. Ross, and P. A. Christiansen, *Int. J. Quant. Chem.*, **40**, 829 (1991).
28. S. A. Wildman, G. A. DiLabio, and P. A. Christiansen, *J. Chem. Phys.*, **107**, 9975 (1997).
29. K. Balasubramanian, *Chem. Rev.*, **89**, 1801 (1989).
30. W. C. Ermler, Atomic HF Program for *jj* coupling scheme.
31. P. Schwerdtfeger, *Inorg. Chem.*, **30**, 1660 (1991).
32. G. Treboux and J. Barthelat, *J. Am. Chem. Soc.*, **115**, 4870 (1993).
33. E. van Lenthe, J. G. Snijders, and E. J. Baerends, *J. Chem. Phys.*, **105**, 6505 (1996).
34. P. Schwerdtfeger, *Phys. Script.*, **36**, 453 (1987).
35. P. Hafner and W. H. E. Schwarz, *J. Phys. B.*, **11**, 217 (1978).
36. W. Kuchle, M. Dolg, H. Stoll, and H. Preuss, *Mol. Phys.*, **74**, 1245 (1991).
37. K. G. Dyall, *J. Chem. Phys.*, **96**, 1210 (1992).
38. P. Schwerdtfeger, H. Silberbach, and B. Miehlich, *J. Chem. Phys.*, **90**, 762 (1989).
39. U. Steinbrenner, A. Bergner, M. Dolg, and H. Stoll, *Mol. Phys.*, **82**, 3 (1994).
40. K. G. Dyall, P. R. Taylor, K. Fægri Jr., and H. Partridge, *J. Chem. Phys.*, **95**, 2583 (1991).
41. P. Pyykkö, *Chem. Rev.*, **97**, 597 (1997).
42. K. P. Huber and G. Herzberg, *Molecular Spectra and Molecular Structure IV: Constants of Diatomic Molecules*, Van Nostrand Reinhold, New York, 1979.
43. P. Schwerdtfeger, P. D. W. Boyd, G. A. Bowmaker, H. G. Mack, and H. Oberhammer, *J. Am. Chem. Soc.*, **111**, 15 (1989).
44. K. Kimura, S. Katsumata, Y. Achiba, T. Yamazaki, and S. Iwata, *Handbook of HeI Photoelectron Spectra of Fundamental Organic Molecules*, Japan Scientific Societies Press, Tokyo, 1980.
45. G. Jonkers, C. A. De Lange, and J. G. Snijders, *Chem. Phys.*, **69**, 102 (1982).
46. S. Roszak, M. Vijayakumar, K. Balasubramanian, and W. S. Koski, *Chem. Phys. Lett.*, **208**, 225 (1993).
47. Y. K. Han, S. Y. Lee, S. J. Park, and Y. S. Lee, unpublished results.
48. J. C. Green, M. L. H. Green, P. J. Joachim, A. F. Orchard, and D. W. Turner, *Phil. Trans. A*, **268**, 111 (1970).